Pulse-pileup correction of signals from a pyroelectric detector for phase-insensitive ultrasound computed tomography (piUCT).

Christian Baker[1], Robert Eckersley[1], and Bajram Zeqiri[2]

[1]King's College London
[2]National Physical Laboratory

January 26, 2018

Abstract

Pellentesque tincidunt lobortis orci non venenatis. Cras in justo luctus, pulvinar augue id, suscipit diam. Morbi aliquet fringilla nibh, vel pellentesque dui venenatis eget. Orci varius natoque penatibus et magnis dis parturient montes, nascetur ridiculus mus. Donec ultricies ultrices magna gravida porta.

Introduction

Ultrasound is typically detected using piezoelectric sensors which respond proportionally to instantaneous acoustic pressure. Such sensors are widely employed in ultrasonic metrology, requiring that values for acoustic intensity and other derived parameters (e.g. power, thermal indices), which cannot be measured directly with a piezoelectric detector, be estimated from measurements of acoustic pressure [1]. When piezoelectric sensors are applied to quantitative medical ultrasound and ultrasound imaging - particularly acoustic attenuation mapping using through-transmission ultrasound computed tomography (UCT) - phase aberration due to inhomogeneity in the density and speed of sound of the medium can result in phase variation over the finite-area of the receiving element [2, 3, 4]. The phase-sensitive receiver will therefore underestimate the acoustic pressure due to phase cancellation across the sensor face. In the case of UCT, this results in artefacts in the reconstructed attenuation map [4, 5, 6]. Sensors that allow direct, phase-insensitive measurement of acoustic intensity are therefore desirable for metrological purposes and also have applications in medical imaging and quantitative ultrasound [4, 5, 6].

At the onset of ultrasound, the rate of change of temperature of an absorbing surface perpendicular to the direction of propagation is directly proportional to the acoustic intensity incident on the surface [7]. A few techniques utilise this for metrological [7, 8, 9] and medical [6] applications. These techniques are potentially useful for medical imaging [4], [6] due to their phase-insensitivity, but each measurement is typically seconds in length - too slow for application in a clinical setting, where thousands of measurements must be made in order to complete a scan. When applied to UCT in a laboratory setting, where speed and sensitivity were not critical, a novel phase-insensitive pyroelectric sensor was shown to be capable of generating quantitative, near artefact-free images of the acoustic attenuation of cylindrical phantoms [4], without employing computational intensive full-wave inversion reconstruction techniques.

Recent improvements to the sensor design and electronics have shortened the response time of the pyroelectric sensor by two orders of magnitude, bringing the technology closer to suitability for clinical application. The new, large area pyroelectric detector forms part of a prototype phase-insensitive UCT (piUCT) scanning platform for through-transmission attenuation imaging of breasts. The main barriers to clinical applicability are measurement rate, dynamic range requirements and maximum measurable attenuation. Increasing the measurement rate further results in pulse-pileup, stopping direct measurement of pulse amplitude. The dynamic range of the measurements can be managed by changing the ultrasound pulsing regime during a scan, resulting in varying pulse shapes in a sequence of piled-up pulses. The maximum measurable attenuation can be improved by increasing the measurement rate (allowing more repeat measurements) and with digital signal processing for noise reduction.

This paper describes a modified maximum likelihood estimation (MLE) pulse-pileup correction method for sequences of closely spaced pyroelectric pulses with varying pulse shapes. The performance of the method was assessed for determining the amplitudes of pyroelectric pulses acquired using the piUCT system. The method was tested using three types of signal: stand-alone pulses, sequences of piled-up pulses with a constant pulse shape, and sequences of piled-up pulses with varying pulse shapes. The method was assessed in combination with stationary frequency domain and dynamic wavelet domain Wiener filtering methods for non-stationary noise reduction.

Background

Phase Insensitive Pyroelectric Sensor

The piUCT sensor exploits the pyroelectric response induced in a thin membrane of polyvinylidene fluoride (PVDF) - a piezoelectric polymer - to detect heating due to attenuation of incident ultrasound. The concept was originally developed for use in a solid-state ultrasound power meter [7]. The membrane is sputtered with gold electrodes on either side, and is effectively a capacitor that charges in response to a change in temperature, and discharges shortly afterwards due to leakage current between the electrodes [10]. In order to maximise the temperature change generated by the ultrasound and therefore the pyroelectric output, the membrane is laminated onto a highly acoustically absorbent polyurethane (PU) backing material. Incident ultrasound passes through the PVDF and is then absorbed by the backing material, heating the PU a short distance (¡ 1 mm) from the PVDF membrane. This heat is conducted back to the PVDF, inducing a pyroelectric voltage response which is proportional to the acoustic power at the membrane-backing interface for a short time after the onset of ultrasound [7].

To facilitate a shorter measurement duration, the leakage current can be varied by changing the impedance with which the sensor is terminated [10]. For the conditions employed in the current piUCT system, the time taken for the onset response $f_o\left(t\right)$ to reach a peak is typically 5 to 10 ms, and the length of the whole onset response is typically ¡ 100 ms. Assuming a single-frequency acoustic field, only the amplitude changes with applied acoustic power, while the shape of the onset response remains constant [8]. The end of an incident single-frequency ultrasound burst of length τ results in a second, inverse pyroelectric response $f_o\left(t\right) = -f_o\left(t-\tau\right)$ due to cooling of the PVDF membrane. For short bursts of ultrasound, the onset and cessation responses are superimposed, resulting in a lower amplitude bipolar pulse waveform characterised by a fast leading edge and a slow trailing edge, and frequency content up to approximately 1 kHz. The pulse length can be shortened with a high pass filter, sacrificing signal amplitude. piUCT uses ultrasound bursts between 1 and 6 ms long, resulting in a pyroelectric pulse that is 10 to 50 ms long. Any subsequent bursts of ultrasound received before the end of the pulse result in pulse pileup – superimposition of subsequent pulses onto the trailing edge of the previous pulse.

Requirements of piUCT Scanning

The piUCT system utilises a 14 element array of 3.2 MHz plane-piston, 10 mm diameter ultrasound transmitters which are scanned over the breast in a parallel-beam tomographic configuration, with the aim of generating a quantitative map of the acoustic attenuation of the tissue. The sensor is large enough to cover the whole field of view of the system, and therefore does not need to be scanned.

After attenuation by the breast, the received acoustic power can be up to 3 orders of magnitude lower than transmitted [**?**]. Signal processing techniques were therefore developed with the aim of resolving low-amplitude pyroelectric amplitudes with a maximised signal to noise ratio and therefore minimised uncertainty.

Sources of noise include: environmental vibration and airborne sound coupled into the water tank, which is detected piezoelectrically; and electromagnetic noise/interference (EMI) emitted from electrical equipment. The sensor has a second pyroelectric membrane laminated behind the backing material, which is acoustically shielded from the ultrasound signal but not from piezoelectric noise, and therefore can act in a differential mode to reduce noise. The second membrane can also act as a noise reference sensor. A copper membrane is laminated to the front of the sensor to shield it from EMI.

It is desirable to minimise the scan duration in order to reduce the likelihood of patient movement and improve patient comfort. The second aim of applying signal processing was therefore to accurately resolve the amplitude of pulses received in quick succession, correcting for the effect of pulse pile-up. The difference in the time of flight of the ultrasound bursts is short enough compared to the pyroelectric response time (µs compares to ms) that arrival times can be accurately estimated from the known transmit time and transmitter-receiver separation.

In order facilitate accurate acquisition of the signals in a received set of piled-up responses, it was necessary to reduce the differences in the amplitude of pulses received in quick succession. This was achieved by transmitting shorter ultrasound bursts along scan lines with a low expected acoustic attenuation, and longer bursts along scan lines with a high expected acoustic attenuation. Reducing the ultrasonic burst length changes the shape of the received pyroelectric pulse, so it was required that a pulse pile-up correction method could resolve the amplitude of pulses with different known pulse shapes.

Filtering

The first aim of applying signal processing techniques to the pyroelectric signals was to maximise the signal to noise ratio and therefore minimise the mean square error in the measurement of the amplitude A of an observed pulse $y\left(t\right)$ in noise. The arrival time of the pulse and its waveform $f\left(t\right)$ were known, but the observed signal had been corrupted by noise $n\left(t\right)$:

$$y\left(t\right) = Af\left(t\right) + n\left(t\right) \tag{1}$$

An optimal filtering approach is the Wiener filter, which is designed in the frequency domain to maximise the ratio of the signal power to the noise power over the length of the signal, rather than the signal to noise ratio at the peak of the signal [11, 12]. The filter $W(\omega)$ is designed to selectively attenuate each frequency band of the input signal according the ratio between the power in the expected waveform with power spectral density $P_y(\omega)$ and the expected noise with power spectral density $P_n(\omega)$ in the same band [12]:

$$W(\omega) = \frac{P_y(\omega)}{P_y(\omega) + P_n(\omega)} \tag{2}$$

For non-stationary signals or noise, where the frequency content of one or both varies with time, a time-varying Wiener filter can be implemented utilising either the short-time Fourier transform [13] or the wavelet transform [14], rather than a discrete-time Fourier transform.

Pulse Pileup Correction

A sequence $y(t)$ of pulses with normalised waveform shapes $f(t)$ corrupted by noise $n(t)$ can be presented as

$$y(t) = \sum_{i=1}^{N} A_i f(t - \tau_i) + n(t) \tag{3}$$

where A_i is the unknown amplitude of the i^{th} pulse, τ_i is its known arrival time and N is the number of pulses in the sequence [15]. Pulse amplitude can be measured directly or using a matched filter, providing that the gap between the start of each pulse is longer than the autocorrelation of the pulse - otherwise, errors are introduced due to the superimposition of the signals [16, 15].

A heuristic method for separating a pulse from pileup is to extrapolate the pulses that precede it, and then subtract the extrapolations from the pulse of interest [17]. Error in the estimation of the amplitudes of preceding pulses will contribute to the error in the estimation of the amplitude of the pulse of interest, resulting in an error that worsens for pulses further into a sequence, which is a problem for piUCT signals.

The amplitudes of piled-up pulses can determined by deconvolution of the known pulse shape from the pulse sequence [15, 17]. This may require amplification of frequency bands containing little or no signal, introducing noise [17]. The deconvolution filter should therefore be designed to reduce the length of the pulses using the available bandwidth. An optimal filter can be designed using a Wiener deconvolution method, taking into account the signal-to-noise ratio is each frequency band of the original signal [15]. The amount by which the pulse length can be shortened is therefore ultimately limited by the spectral content of the original signal, and in practice may not provide the best possible estimate of pulse amplitude [15].

A maximum-likelihood estimate of the amplitudes of piled-up pulses can be derived, for which the probability of obtaining the set of amplitudes is largest [15, 18, 19]. The maximum likelihood estimate of the set of N amplitudes A of the received overlapping pulses in equation 3 can be calculated using the following vector equation:

$$A = \Lambda^{-1}\Phi \tag{4}$$

where Λ is the matrix described by

$$\Lambda = \begin{bmatrix} \lambda_{11} & \dots & \lambda_{1N} \\ \dots & \dots & \dots \\ \lambda_{N1} & \dots & \lambda_{NN} \end{bmatrix} \tag{5}$$

each element λ_{ij} of Λ is

$$\lambda_{ij} = \int_{t=0}^{T} f\left(t-\tau_i\right) f\left(t-\tau_j\right) dt \tag{6}$$

and the i^{th} element of the column vector Φ is

$$\Phi_i = \int_{t=0}^{T} y\left(t\right) f\left(t-\tau_i\right) dt \tag{7}$$

This method allows the determination of the amplitudes of closely-spaced pulses irrespective of spectral content, and forms the basis of the method used for pulse pileup correction of pyroelectric signals from the piUCT system.

1 Experimental Methods

All signal processing algorithms were written in the Python programming language (version 2.7), and applied to digitally-stored signals acquired using the NPL piUCT system.

A modified Maximum Likelihood Estimation (MLE) pulse pileup correction method was implemented for the determination of the amplitude of the underlying onset and cessation responses that constituted an individual pyroelectric pulse, or sequence of piled-up pulses. The amplitudes of the underlying responses were independent of the length of the ultrasonic bursts that induced each pulses, providing a measurement of the continous-wave equivalent acoustic power at the onset and cessation of the bursts respectively.

Each pulse $f\left(t\right)$ was approximated as the sum of an onset response $s\left(t\right)$ and a cessation response $-s\left(t\right)$, with the each cessation response delayed relative to the onset by the known length l_i of the ultrasound burst that induced the i^{th} pulse. The waveform shape of the i^{th} received pulse is therefore written as:

$$f_i\left(t\right) = s\left(t\right) - s\left(t-l_i\right) \tag{8}$$

This was then substituted in to equations 6 and 7 before carrying out the MLE as described in equations 4 and 5.

The performance of the method was tested using three types of signal acquired from the piUCT system: stand-alone pulses, sequences of piled-up pulses with a constant pulse shape, and sequences of piled-up pulses with varying pulse shapes. Each signal type was acquired multiple times at various transmitted acoustic powers. This length was chosen to be short enough relative to thermal time-scales to not induce its own pyroelectric response. Pulse amplitudes were determined separately with up to three prefiltering conditions: directly after acquisition (no prefiltering); after prefiltering with a stationary with a stationary frequency-domain Wiener filter (FDWF); and after prefiltering with a time-varying wavelet-domain Wiener filter (WDWF) (Daubechies 1 wavelet). Means and coefficients of variation were determined from the repeat measurements of each combination of signal type, prefiltering condition and acoustic power.

For both piled-up signal types, 14 bursts were transmitted with a period of 8 ms. This simulated the burst regime that the piUCT system utilises in practice, with one burst transmitted out of each of the fourteen transducer array elements. For all signal types, the acoustic output power was varied by changing the duty cycle of the signal within each burst, maintaining a 10 cycle 'sub-burst' length.

For the acquisition of the test signals, the piUCT sensor and transducer array were positioned in the piUCT water tank with a separation of 65 mm. The transducer drive level was set so as to generate a continuous-wave acoustic output power of approximately 20 W. The same array element was used for all measurements so that the differing efficiencies of the elements would not affect results. The separation distance and acoustic output power were both chosen so as to minimise the generation of harmonics due to non-linear propagation. The resulting acoustic field at the transducer face contained a 2nd harmonic amplitude ? dB below the level of the fundamental component.

The template signal $s(t)$ was generated by averaging 250 measurements of the onset response of the sensor, and smoothing the averaged waveform with a 3rd order Savitsky-Golay filter. The onset response was isolated from the cessation response using a long (500 ms) burst.

Noise estimates for the Wiener filter were obtained using the sensor's reference membrane signal, and clean signal estimates were created using the template signal and the amplitude determined from direct measurement.

Individual Pulses

Individual pyroelectric pulses induced by 6 ms long bursts of ultrasound transmitted at 7 different acoustic powers between 14% and 88% of the maximum output power were acquired, with 250 repeat measurements made at each power. The burst length was chosen to be longer than the time-to-peak of onset response, so that the pulse amplitude was equal to the underlying onset response amplitude, and the results could be used as ground-truth value for amplitudes determined from piled-up sequences.

The pyroelectric amplitudes of the unprocessed, FDWF and WDWF signals were estimated by direct amplitude measurement and MLE. The mean amplitude values obtained from direct measurement of the unprocessed signals were taken as the ground-truth amplitudes. The coefficient of variation of the 6 methods was compared, as well as the bias of the 5 processed methods compared to the ground-truth direct measurement.

Fixed Shape Piled-up Pulse Sequences

Fixed shape pulse sequences were generated using 4 ms ultrasound bursts. 50 repeat measurements were made at each of 49 output powers between 2% and 98% of the continuous wave output power. The MLE method was used to estimate the underlying onset response amplitudes in the resulting signals with and without processing by the WDWF. The FDWF was not used because it performed poorly compared to the WDFW on measurements of individual pulses. The clean signal estimates required by the WDWF were generated using the template signals, and the amplitudes determined from MLE of the unprocessed signals.

The coefficient of variation of the results were compared, as well as the bias against ground-truth values determined from a linear fit to the individual pulse amplitudes described above.

Varying Shape Piled-up Pulse Sequences

The MLE method was tested on piled-up signals induced by an ultrasound burst sequence with varying burst lengths. The same procedure was used as for the fixed shape piled-up pulses sequences, but for each set of 50 repeat measurements, 14 burst lengths were chosen at random between 1 ms and 4 ms (rounded to the nearest 10 cycles). The burst period was kept constant at 8 ms. Processing and analysis was carried out in the same manner as for the fixed shape piled-up pulse sequences.

Results

The template signal that was used for Wiener filtering and MLE processing is shown in figure 1, plotted with a representative individual pyroelectric pulse, generated using a 6 ms ultrasound burst. The cessation response, which occurred 500 ms into the signal, has been inverted and shifted by -500 ms so that it is plotted on top of the onset response, demonstrating the equivalence of their shape. The difference in the amplitudes of the two signals was less than 0.11 dB.

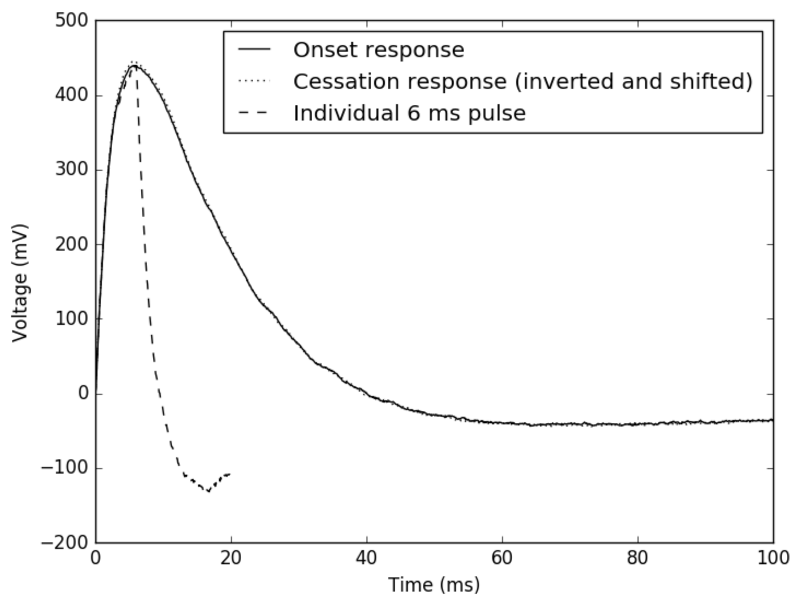

Figure 1: Average of 250 measurements of the onset $f_0(t)$ and cessation $f_c(t) = -f_o(t-\tau)$ response of the sensor at the maximum transmitted power, and the average of 50 measurements of an individual pyroelectric pulse generated using a 6 ms ultrasound burst at maximum power. The cessation response has been inverted and shifted by -τ so that its amplitude can be compared with that of the onset response.

Individual Pulses

Figure 2 shows the bias in the measurement of the amplitude of the individual pulses using 5 processing methods: frequency domain Wiener filtering (FDWF); wavelet domain wiener filtering (WDWF); maximum likelihood attenuation (MLE); MLE after prefiltering with FDWF; and MLE after prefiltering with WDWF. Bias was calculated relative to the ground-truth. Pulse amplitudes determined using MLE without prefiltering suffered from no significant bias, whereas both Wiener filtering techniques caused an underestimation in pulse amplitude that worsened as the signal amplitude decreases. The dynamic WDWF performed better than the stationary FDWF.

The coefficients of variation of the individual pulse measurements are shown in Figure 3. The FDWF showed only a marginal improvement over direct amplitude measurement. Coefficients of variation of WDWF measurements were much lower than those of the direct and FDWF measurements, demonstrating the effectiveness of using a dynamic filter over a stationary one in the presence of time-varying signals and noise. However, MLE without prefiltering was the best performing technique.

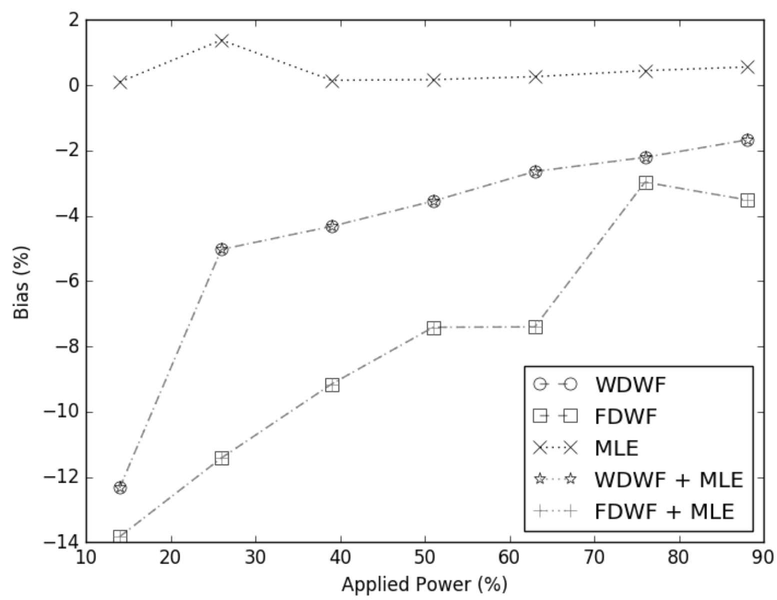

Figure 2: Bias of Wiener filter and MLE measurements of amplitude relative to the ground-truth amplitudes measured directly.

Fixed Shape Piled-Up Pulse Sequences

Figure 4 shows the bias of the MLE measurements, with and without pre-processing with a WDWF, relative to the ground-truth values. Both methods underestimate the pulse amplitude significantly, but the WDWF caused the underestimation to worsen for lower amplitude signals. The coefficient of variation of the MLE measurements with and without WDWF prefiltering are shown in Figure 5, along with the coefficient of variation of the amplitudes of the first pulses in the sequences, measured directly, with and without WDWF filtering. When the amplitude was measured directly (without pulse pile-up), WDWF provided a significant improvement compared to measurement of the raw pulse amplitudes. MLE pulse pile-up correction performed better still, however, with the WDWF prefiltering making no discernible difference to the coefficient of variation of the MLE technique.

Varying Shape Piled-Up Pulse Sequences

Figure 6 shows the bias of the MLE amplitude measurements of piled-up pulse seqeunces of pulses with

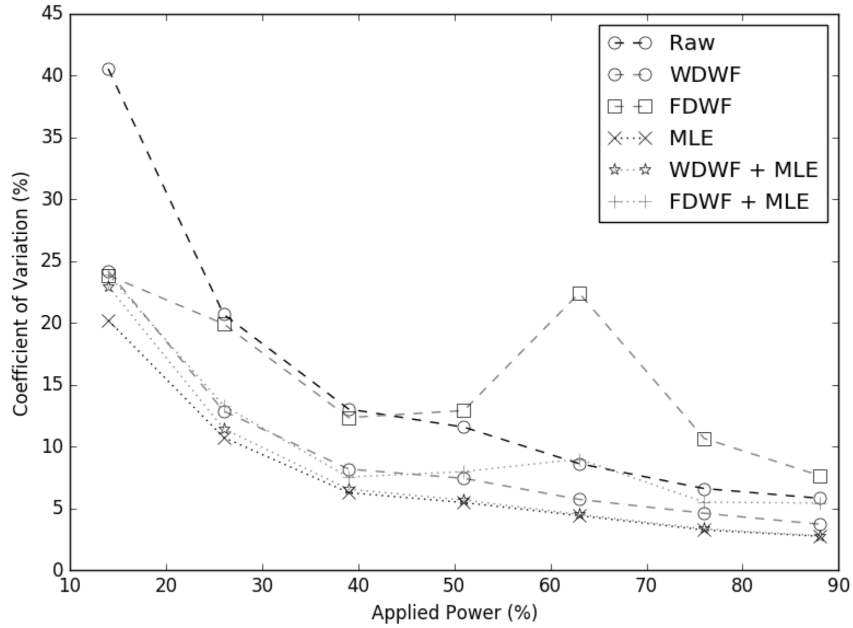

Figure 3: Coefficient of variation of direct and MLE measurements of the amplitude of pyroelectric signals without pileup, with and without Wiener filtering.

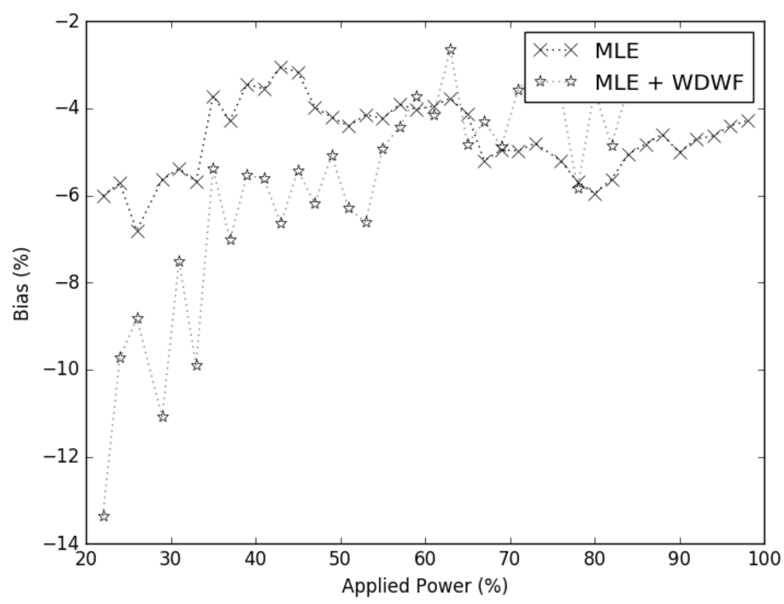

Figure 4: Bias of the mean pyroelectric amplitudes determined from MLE processing of 4 ms on, 4 ms off piled-up sequences relative to the ground truth, with and without pre-processing with a wavelet domain Wiener filter

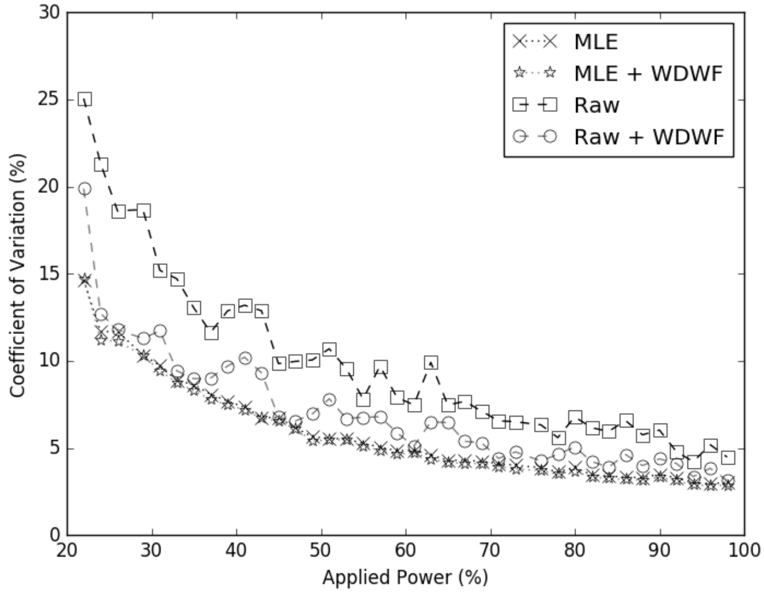

Figure 5: Coefficient of variation of the pyroelectric amplitudes determined from direct measurement of the amplitude of the first pulse in the sequence ('Raw'), and from MLE processing, of 4 ms on, 4 ms off piled-up sequences, with and without pre-processing with a wavelet domain Wiener filter

varying pulse shape, generated through randomisation of the ultrasound burst length. Bias was calculated relative to ground truth values determined from direct measurement of individual pyroelectric pulses. The MLE pulse-pileup correction underestimated the pulse amplitude both with and without preprocessing with a WDWF, but performs better without preprocessing. The coefficient of variation of the MLE and direct amplitude measurements, with and without pre-processing, are shown in Figure 7. As was seen for the fixed shape pulse seqeunces, while a WDWF improves the coefficient of variation for direct amplitude measurement, no discernible difference is seen when the signal is preprocessed with a WDWF prior to MLE pulse pile-up correction. MLE without preprocessing shows the lowest variation.

Discussion

Figure 2 shows that both the frequency domain Winer filter (FDWF) and wavelet domain Wiener filter (WDWF) caused a bias to the measurement of pyroelectric pulses without pileup, underestimating the amplitude. The FDWF will have smoothed the discontinuities in the signals that occurred at switch-off, resulting in a reduced amplitude, causing the bias on the direct amplitude measurements of the FDWF signals. Although the FDWF filter kernel was applied to the template signal before it was used for MLE processing, the discontinuities are only manifested from pile-up and are therefore no present in the template signal. This is a likely cause of the bias in the MLE + FDWF results. The WDWF will have also smoothed discontinuities. However, the WDWF was dynamic, altering its characteristics as a function of time based on comparison of the signal and noise reference. It was therefore not possible to process the template waveform with the WDWF filter kernel before MLE processing. The change in amplitude of the signals due to the WDWF was

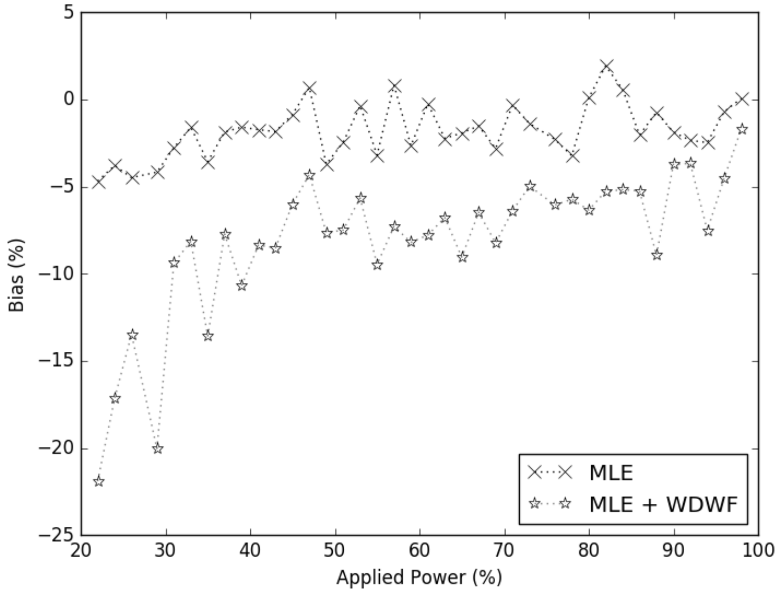

Figure 6: Bias of pyroelectric amplitudes of randomised burst length pulse sequences, with and without pre-processing, relative to ground truth values.

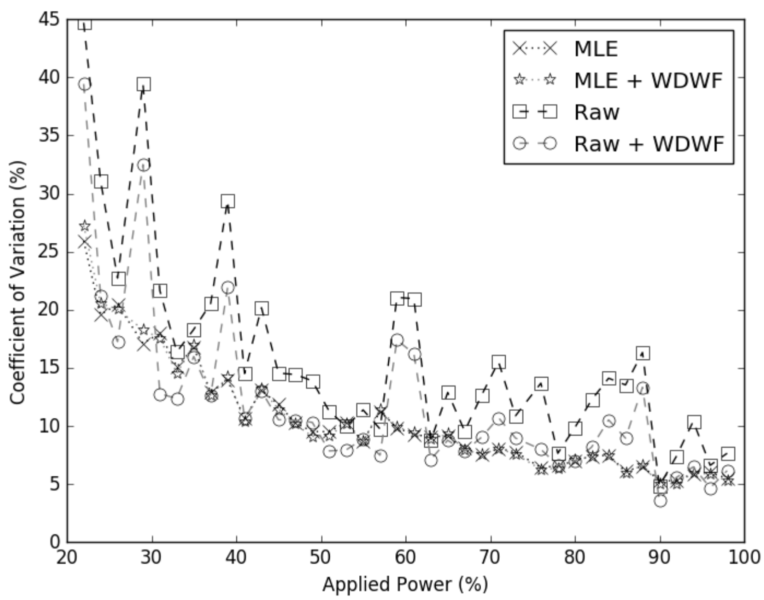

Figure 7: Coefficient of variation of the pyroelectric amplitudes determined from direct measurement of the amplitude of the first pulse in the sequence ('Raw'), and from MLE processing, of randomised burst length piled-up sequences, with and without pre-processing with a wavelet domain Wiener filter

therefore not compensated for, causing the bias seen in the MLE + WDWF data. The bias in the amplitudes determined through MLE with no pre-processing filter was small, with the exception of one point at low applied power, which was likely affected by a poor signal-to-noise ratio.

The coefficients of variation of the measurement of pyroelectric pulses without pileup are presented in figure 3. Processing of the signals with the FDWF before direct amplitude measurement shows no improvement in measurement accuracy over direct measurement of the raw signals. This was likely due to the dynamic nature of the noise, which had to be approximated as a stationary noise power for FDWF processing. Pre-processing with the WDWF, however, resulted in between 3 and 9 percentage points of improvement demonstrating the benefit of dynamic filters in the presence of dynamic noise. However, pre-processing with WDFW provided no improvement to the accuracy of MLE measurement, and pre-processing with the FDWF actually worsened the performance of MLE. Although the MLE measurement requires no estimate of the noise, it has an inherent resistance even to dynamic noise, and is superior to direct measurement of the amplitudes after pre-processing with an optimum dynamic Wiener filter. This is likely a manifestation of the fact that Wiener filtering performs optimisation of the shape of its output compared to the desired output, rather than the amplitude of the pulse [15]. When the shape of the expected signal is known with high certainty, as is true for the measurement of pyroelectric signals with no pileup, MLE is superior.

As expected from measurement of signals without pile-up, the WDFW introduced a measurement bias for both fixed and varying pulse shape sequences. However, figures 4 and 6 show that MLE underestimated the pyroelectric amplitude even without the WDWF in both cases. No such bias was present on the MLE measurement of signals with no pileup in figure 2. This underestimate may indicate that the assumption that the sequences of pyroelectric pulses result in linear superimposition is invalid, due to different initial thermal conditions of the sensor if signal is detected during cooling or when the sensor is in a steady state.

Figure 5 compares the mean coefficient of variation of the amplitude of all 14 pulses as determined using MLE with the coefficient of variation of the amplitude of only the first pulse in the sequence measured directly. Direct amplitude measurement could not be applied to all pulses, because of the pulse pile-up, and therefore results of direct measurement of signals filtered with the FDWF and WDWF are not included. The results demonstrate that the coefficient of variation of MLE measurements is better than that of direct amplitude measurement, and that pre-processing with a WDWF shows no improvement, as expected from the results of measurements of signals without pile-up. The coefficient of variation was worse for the piled-up signals than the individual signals, because a shorter burst length was used, resulting in a lower pyroelectric amplitude and therefore poorer signal-to-noise ratio.

Figure 7 compares the coefficients of variation in the same manner as figure 5 for piled-up signals with variable burst length. The results vary between applied powers because the randomised burst lengths will have resulted in changes to the pyroelectric amplitude and therefore the average signal-to-noise ratio across the 14 pulses in the train for each applied power. However, in general, the results match with those previously discussed – MLE is superior to direct amplitude measurement, with no benefit in pre-processing with WDWF.

The template signal shown in figure 1 is only valid for single-frequency ultrasound fields. At higher acoustic pressures, or with a longer separation between the transmitter array and sensor, the onset response of the sensor was reduced in amplitude relative to the cessation response, and therefore the template signal shown in figure 1 was no longer valid.

This is likely due to the presence of harmonics in the acoustic field, generated by a combination of nonlinear propagation and nonlinearities in the transmitter drive system and the transmitters themselves. Higher frequency ultrasound is more readily absorbed by the backing material of the sensor, causing a faster rate of change of temperature during heating. For this reason, the sensitivity of the sensor increases with frequency [8]. It is possible that if harmonics are present in the acoustic field, the derivative of the rate of heating might have a different shape due to the different penetration depths of the harmonics into the absorbing backing material of the sensor, causing a different pyroelectric response shape. The rate of cooling, however, would not be affected by the harmonic content of the field, as it is dependent only on the difference between the sensor temperature and the water temperature at the time of cessation. This will be the subject of a follow-up study.

If a template signal acquired in a single-frequency field is used for MLE processing of pyroelectric pulse sequences acquired in a nonlinear field, which could occur during parts of a piUCT scan, then the accuracy of the resulting amplitudes will suffer. The error introduced has yet to be quantified. This could be compensated for through characterisation of the frequency response of the sensor, and inclusion of a function that modified the template signal based on an initial estimate of the acoustic power and therefore harmonic content of the signal. This could potentially be reversed, allowing estimation of the harmonic content of the signal from the pyroelectric pulse shape. Alternatively, the piezoelectric response of the sensor could be used to measure the harmonic content of the signal, and the resulting values could be corrected accordingly.

Conclusion

Digital processing methods for the determination of the amplitude of signals from a pyroelectric ultrasound sensor in the presence of time-varying noise and pulse pile-up were compared, for application to phase-insensitive ultrasound computed tomography.

Processing of signals with a dynamic wavelet-domain Wiener filter before amplitude measurement resulted in improved measurement accuracy compared to direct amplitude measurement of the raw signals, as well as to measurement after processing with a stationary frequency-domain Wiener filter. However, a maximum-likelihood estimation method, which required knowledge of the shape of the expected waveform with high certainty, proved to be superior to direct amplitude measurement of the dynamically filtered signals, and pre-processing of the signals with the dynamic filter before maximum likelihood estimation showed no improvement.

A modified maximum-likelihood method was developed that could determine the underlying amplitudes in a sequence of piled-up signals with variable pulse-lengths due to varying burst lengths of the incident ultrasound. It was demonstrated that the method was capable of accurately measuring pyroelectric amplitudes and therefore incident acoustic power, with a high resilience to noise. No improvement was seen when signals were pre-processed with a dynamic Wavelet-domain Wiener filter.

The methods were tested on single-frequency acoustic fields, where it could be assumed that the shape of the pyroelectric response of the sensor remained constant with applied power. In practice, harmonics generated through nonlinear propagation are likely, and therefore this assumption will not hold. Future work will investigate the effect of a harmonically-rich field on the sensor's pyroelectric response, and develop methods to determine the amplitudes of piled-up signals detected in such a field.

References

[1] R. C. Preston, *Output Measurements for Medical Ultrasound*. 1991.

[2] P. L. Carson and A. Fenster, “Anniversary paper: evolution of ultrasound physics and the role of medical physicists and the AAPM and its journal in that evolution.,” *Medical Physics*, vol. 36, no. 2, pp. 411–428, 2009.

[3] L. M. Hinkelman, D. L. Liu, R. C. Waag, Q. Zhu, and B. D. Steinberg, “Measurement and correction of ultrasonic pulse distortion produced by the human breast.,” *The Journal of the Acoustical Society of America*, vol. 97, no. 3, pp. 1958–1969, 1995.

[4] B. Zeqiri, C. Baker, G. Alosa, P. N. T. Wells, and H.-D. Liang, “Quantitative ultrasonic computed tomography using phase-insensitive pyroelectric detectors.,” *Physics in Medicine and Biology*, vol. 58, no. 15, pp. 5237–68, 2013.

[5] L. J. Busse and J. G. Miller, “Response characteristics of a finite aperture, phase insensitive ultrasonic receiver based upon the acoustoelectric effect,” *Journal of the Acoustical Society of America*, vol. 70, no. 5, pp. 1370–1376, 1981.

[6] J. R. Klepper, G. H. Brandenburger, J. W. Mimbs, B. E. Sobel, and J. G. Miller, “Application of phase-insensitive detection and frequency-dependent measurements to computed ultrasonic attenuation tomography.,” *IEEE Transactions on Biomedical Engineering*, vol. 28, no. 2, pp. 186–201, 1981.

[7] B. Zeqiri, P. N. Gélat, J. Barrie, and C. J. Bickley, “A novel pyroelectric method of determining ultrasonic transducer output power: device concept, modeling, and preliminary studies.,” *IEEE Transactions on Ultrasonics, Ferroelectrics and Frequency Control*, vol. 54, no. 11, pp. 2318–2330, 2007.

[8] V. Wilkens, “A thermal technique for local ultrasound intensity measurement: part 1. Sensor concept and prototype calibration,” *Measurement Science and Technology*, vol. 21, no. 11, pp. 115805 – 115813, 2010.

[9] A. Shaw and J. Nunn, “The feasibility of an infrared system for real-time visualization and mapping of ultrasound fields.,” *Physics in medicine and biology*, vol. 55, no. 11, pp. N321–7, 2010.

[10] J. G. Webster and H. Eren, *Measurement, Instrumentation and Sensors Handbook, Second Edition*. 2014.

[11] S. W. Smith, *The Scientist and Engineer’s Guide to Digital Signal Processing*. 1997.

[12] N. Wiener, *Extrapolation, Interpolation, and Smoothing of Stationary Time Series: With Engineering Applications*. 1942.

[13] A. Y. Kostiev, A. Y. Butrym, and S. Shulga, “Time-varying wiener filtering based on short-time fourier transform,” *2012 6th International Conference on Ultrawideband and Ultrashort Impulse Signals*, pp. 305–308, 2012.

[14] M. S. Woolfson, “M S Woolfson, X B,” 1995.

[15] J. E. Ehrenberg, T. E. Ewart, and R. D. Morris, “Signal-processing techniques for resolving individual pulses in a multipath signal,” *The Journal of the Acoustical Society of America*, vol. 63, no. 6, p. 1861, 1978.

[16] V. Radeka and N. Karlovac, "Institute Ruder Bo˜kovi6, Zagreb, Yugoslavia," vol. 52, no. 1, pp. 86–92, 1966.

[17] T. K. Lewellen, "Evaluation of a clinical scintillation camera with pulse tail extrapolation electronics," *J. Nuc. Med.*, vol. 30, no. 9, pp. 1554–1558, 1989.

[18] M. Bolic, V. Drndarevic, and W. Gueaieb, "Pileup correction algorithms for very-high-count-rate gamma-ray spectrometry with NaI(T1) detectors," *IEEE Transactions on Instrumentation and Measurement*, vol. 59, no. 1, pp. 122–130, 2010.

[19] I. J. Myung, "Tutorial on maximum likelihood estimation," *Journal of Mathematical Psychology*, vol. 47, no. 1, pp. 90–100, 2003.